

Direct surface charging and alkali-metal doping for tuning the interlayer magnetic order in planar nanostructures

Tamene R. Dasa and Valeri S. Stepanyuk

Max-Planck-Institut für Mikrostrukturphysik, Weinberg 2, D-06120 Halle, Germany

The continuous reduction of magnetic units to ultra small length scales inspires efforts to look for a suitable means of controlling magnetic states. In this study we show two surface charge alteration techniques for tuning the interlayer exchange coupling (IEC) of ferromagnetic layers separated by paramagnetic spacers. Our *ab-initio* study reveals that already a modest amount of extra charge can switch the mutual alignment of the magnetization from anti-ferromagnetic to ferromagnetic or vice versa. We also propose adsorption of alkali metals as an alternative way of varying the electronic and chemical properties of magnetic surfaces. Clear evidence is found that the interlayer magnetic order can be reversed by adsorbing alkali metals on the magnetic layer. Moreover, alkali metal overlayers strongly enhance the perpendicular magnetic anisotropy in FePt thin films. These findings combined with atomistic spin model calculations suggest that electronic or ionic way of surface charging can have a crucial role for magnetic hardening and spin state control.

I. INTRODUCTION

Efficient ways of manipulating memory units and logic devices became an emergent motive in the field of spin electronics^{1,2}, in addition to minimizing their sizes. In the last few decades the reading scheme of the modern hard disc drive was reduced to the nanoscale level following the discovery of giant magnetoresistance effect in metallic multilayers by Grunberg and Fert^{3,4}. Current technology uses tunneling magnetoresistance for reading the state of magnetic units^{5,6}. It relies on the relative alignment of the magnetic layers interspaced by coupling medium, which results in the difference of the tunneling resistance. The existence of such intriguing characteristics is related to the delocalized electrons within the coupling medium that are confined. Apart from the advancement in the reading mechanism of the state of the magnetic units, the writing head still makes use of magnetic field which has less capability of controlling magnetic states on short length scales. Alternatively, such magnetic states can be reversed using the current-induced-spin transfer torque technique in which the spin-polarized current tunnel through the junction and consequently producing spin-torque^{7,8}. It has also been shown that the mutual magnetization in magnetic tunneling junction can be tuned by applying a voltage and this effect has similar order of magnitude like that of spin transfer torque^{9–11}.

Recently a more efficient method has been revealed, on the basis of magnetoelectric coupling, for tuning the spin alignment in a ferromagnet (FM) by both Density Functional theory^{12–16} and experimental studies^{1,17,18}. For instance, the anisotropy properties of 2D ferromagnet could be tuned either by varying its intrinsic charge carriers^{12,15} or the oxidation state by electric means¹⁹. On the other, hand external electric field was used in combination with multiferroic materials to reverse the relative alignment of ferromagnets separated by non-magnetic medium (FM/NM/FM)^{20–22}. Theoretical studies have shown that the interlayer exchange coupling and

magnetoresistance effect are inter-related^{23,24}. Nonetheless, direct manipulation of the interlayer exchange coupling is one of the feasible and perhaps the least investigated approaches for a tuning magnetic order. It would even be more compelling to find a possible way of tuning magnetic coupling or anisotropy in planar nanostructures with ionic doping.

Our study verifies a possible route for manipulating the IEC and the relative alignment of the magnetic layers interspaced by non-magnetic multilayers, employing direct surface charging and alkali metal adsorption. The former mechanism relies on sequential variation of the intrinsic charge concentration of FM/NM/FM multilayer, and the results related to this phenomena are presented in Sec. III. Additionally, in Sec. IV we propose that the process of surface charge alteration can be accomplished by adsorbing free-electron systems, alkali metals, on surfaces. Indeed, this mechanism alters the electrochemical features of magnetic surface and leads to reversal of the relative spin alignment. Apart from tuning the interlayer magnetic order the magnetic anisotropy of Fe/Pt multilayer can be significantly enhanced by using alkali metal deposition. To better appreciate such increase of the MAE, in Sec. V the hysteresis loop for FePt multilayer is plotted through the atomistic spin model approach. The discussion and analysis on these findings is presented in Sec. VI, followed by conclusion in Sec. VII.

II. COMPUTATIONAL DETAILS

A thorough *ab-initio* study was performed within the projector augmented wave technique (PAW)²⁵ as implemented in the VASP code^{26,27}. The local spin density approximation (LSDA) is used for the exchange and correlation interactions²⁸. Plane wave basis set is used to describe the Kohn-Sham wave function, and in all calculations the plane wave cut off energy of 430 eV was used. A dense k -point mesh of 21x21x1 and smearing width of 2 meV, that are tested for their reliability, were employed

to obtain a more accurate value of MAE and IEC. We have used a supercell approach in which two layers of Fe separated with finite number of Cu spacers are supported by Pt(001) substrate²⁹. The surface charging effect is introduced by sequentially varying the number of valence electrons. Additionally, a uniform charge background is assumed³⁰. Doping of alkali metals is done by capping the top magnetic layer with two different structures of Na or Li overlayers, namely $p(1 \times 1)$ and $c(2 \times 2)$. For the latter configuration a 2×2 supercell is used. The pairwise exchange coupling or simply the interlayer exchange coupling (E_{IEC}) was calculated as $E_{IEC} = E_{AF} - E_{FM}$, and for all charge states the spins were aligned along their easy axes. For 2×2 supercell the interlayer coupling is calculated as, $E_{IEC} = \frac{1}{4}[E_{AF} - E_{FM}]$. To determine the easy axis of magnetization we have performed a fully-relativistic calculation including spin-orbit coupling³¹. The magnetic anisotropy energy (MAE) is evaluated by taking the energy difference between two axis of magnetization, parallel ([100]) and perpendicular ([001]) to the surface plane. Similar procedure is followed to calculate the MAE for antiferromagnetic configuration and the two spins are oriented anti-parallel to each other for both axis of magnetization. Here after, we shall denote the charge added to the multilayers (net charge) as $q_{+(-)}$ whereas n stands for the charge density of the entire system.

In order to study the magnetization reversal in FePt planar nanostructures, we use atomistic spin model approach.³² It is essential enough to investigate this phenomena by mapping the magnetic properties already investigated on the basis of electronic structure theory with atomistic spin models. In the latter case the energetics of interacting spin with an effective magnetic moment is described by spin Hamiltonian which has a form

$$\mathbf{H} = \sum_{i \neq j} J_{ij} \mathbf{S}_i \cdot \mathbf{S}_j - k_u \sum_i (\mathbf{S}_i \cdot \mathbf{e})^2 - \sum_i \mu_s \mathbf{S}_i \cdot \mathbf{H}_{app} \quad (1)$$

where the first, middle and last terms describe the exchange interaction (H_{exc}), magnetic anisotropy (H_{MAE}) and the external magnetic field (H_{app}) or Zeeman term respectively. J_{ij} is the exchange coupling parameters between atomic sites i and j , and the local spin moments are denoted with unit vector \mathbf{S}_i and \mathbf{S}_j obtained from the realistic atomic moments as $\mathbf{S}_i = m_s/|m_s|$. The exchange coupling parameters and the single ion anisotropy, in Eq. 1, are obtained from calculations on the basis of density functional theory. The magnetization curves are simulated by solving the stochastic Landau-Lifshitz-Gilbert (LLG) equation. At the atomic level the LLG equation is written as

$$\frac{\partial \mathbf{S}_i}{\partial t} = -\frac{\gamma}{(1 + \lambda^2)} \mathbf{S}_i \times [\mathbf{H}_{i,eff} + \lambda(\mathbf{S}_i \times \mathbf{H}_{i,eff})] \quad (2)$$

where $\gamma = 1.76 \times 10^{11} \text{ T}^{-1}\text{s}^{-1}$ is the absolute value of the gyromagnetic ratio, λ is the damping parameter and the atomistic effective magnetic field is denoted with $\mathbf{H}_{i,eff}$. The effective magnetic field is derived from the spin Hamiltonian shown in Eq. 1.³² The FePt multilayers are modeled with two Fe layers separated with an effective medium and it extends as $6 \text{ nm} \times 7 \text{ nm}$ within the xy plane. When simulating the magnetization curve thermal effect and magnetostatic field are taken into consideration that are included in the effective magnetic field^{32,33}. Further discussion on the hysteresis loop of FePt multilayers is presented in Sec. V.

III. SWITCHING INTERLAYER EXCHANGE COUPLING WITH SURFACE CHARGING

First, we present the results concerned with the influence of direct surface charging on the relative magnetization of two magnetic layers separated with Cu spacer. When the charge neutrality of metallic multilayers is perturbed by additional positive or negative charges, it leads to spatial charge re-distribution mainly towards the surface. Whereas, a reduced variation of the spatial charge is also observed underneath the surface. Such charge re-

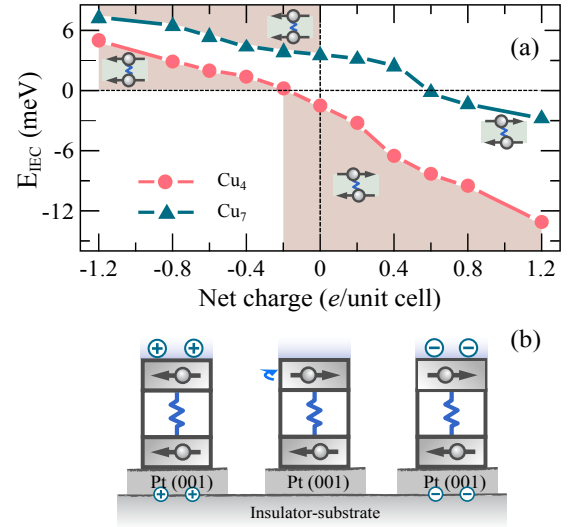


FIG. 1. (Color online)(a) The interlayer exchange coupling (IEC) between the magnetic layers in Fe/Cu_N/Fe multilayers on Pt(001) as function of the net charge in the system. As an illustration such relations are plotted for Cu spacer thickness of $N = 4$ (circle) and $N = 7$ (triangle). (b) A schematic description of Fe/Cu₄/Fe and the relative alignment of the magnetization as result of charge injection or removal.

distribution can even be spin-dependent which can alter the magnetic order^{13,15}. Meanwhile, the exchange interaction across the coupling medium in Fe/Cu_N/Fe trilayer, supported on a Pt(001) substrate, determines the magnetic state to be either ferromagnetic (FM) or antiferromagnetic (AF). For such multilayers we demonstrate

a strong effect of direct surface charging on the relative magnetic order. As an illustration, in Fig. 1 the variation of the interlayer exchange coupling for Fe/Cu_N/Fe multilayers in response to the addition or removal of charges is depicted for Cu spacer thickness of $N = 4$, and $N = 7$ layers. The Fe layers separated with four layers of Cu (uncharged) are coupled antiferromagnetically, and the E_{IEC} is found to be -2.5 meV. The antiferromagnetic coupling can be further enhanced by negative charge doping. As an example, by injecting negative charge of the order of $\Delta q = 1.2 \bar{e}$ per unit cell³⁴ Fe/Cu₄/Fe, the absolute value of the E_{IEC} is increased to 12 meV. The most fascinating finding is observed when the electron concentration is reduced from the neutral Fe/Cu₄/Fe, which results in the switching of the relative magnetic order from antiferromagnetic coupling to ferromagnetic one. Explicitly, switching from AF configuration to FM takes place when the system is charged with $0.2 h$ per unit cell, and further increment of the extra holes to $1.2 h$ per unit cell leads to E_{IEC} of ~ 5 meV.

An essential issue now could be the interplay of finite size effect, *i.e.* thickness of the Cu spacer, surface charging and the interlayer exchange coupling. In order to investigate this phenomena the exchange coupling (E_{IEC}) with respect to charge injection is investigated for thicker Cu layers. In Fig. 1 (a) we have employed seven layers of Cu as mediator in which the IEC of the uncharged system is 3.6 meV. Similar to the case of four layers, here space charge variation has significant effect on the IEC. Addition of certain amount of negative charges switches the magnetic coupling to AF. Interestingly, for Fe/Cu₇/Fe multilayers a transition of the easy axis of magnetization from in-plane to out of plane directions and the reversal of the relative magnetic order are observed at the same charge state, *i.e.* at $0.6 \bar{e}$ /unit cell. In another multilayer, *i.e.* Fe/Cu₆/Fe trilayer, we found that the magnetic moments are counter-aligned for all charge states. But, the influence of negative charge injection on the IEC is much stronger than the positive ones. Precisely, the absolute value of the IEC for the neutral system (~ 6 meV) is reduced by 75 %, as soon as the system is injected with $1 \bar{e}$ per unit cell. One should note that for the experimental realization of effective surface-interface charging the alloy multilayers should be electrically decoupled, by semiconductor or insulator as shown in Fig. 1 (b), and hence the net charge is trapped in the upper layers.

IV. ALKALI-METAL-INDUCED SWITCHING OF THE INTERLAYER MAGNETIC ORDER

So far we have shown the impact of charge injection on magnetic order by controlling the intrinsic charge carriers. Albeit, controlling the number of charge carriers in a slab could be experimentally challenging task. Thus, the efforts looking for an alternative method of varying the surface electronic structure are underway. Recently it was shown that incorporating a net charge

in nanostructure can be achieved by electrolyte^{35–37}, or by adding dopants³⁸, whereas using scanning tunneling microscope or electron force microscope tip is also indispensable option³⁹. Doping of magnetic entities with alkali metals or halogens can lead to a significant variation of the electrochemical properties^{40,41} as well as their spin properties^{42,43}. Moreover, alkali metals are illustrative free-electron systems and have relatively small ionization energies. Here we verify that alkali-metals deposited on magnetic surface can be employed as a natural way of varying the electronic and chemical properties of FM/NM/FM trilayers and the magnetic properties could be controlled therewith. Particularly, the interplay between the deposition of alkali metals and the change in the interlayer magnetic coupling is investigated. In Fig. 2 (a) the values of the IEC for Fe/Cu_N/Fe and Na/Fe/Cu_N/Fe multilayers is presented. The magnetic coupling of Fe/Cu_N/Fe oscillates between FM and AF order as the thickness of the spacer increases, which is related to the quantum well states (QWS) in the Cu multilayers^{23,44}. In fact, the results for six, seven and eight Cu layers of the neutral systems are compared with available studies based on Korringa-Kohn-Rostoker method⁴⁵, and the magnetic order as well as the exchange coupling energies are in a very good agreement.

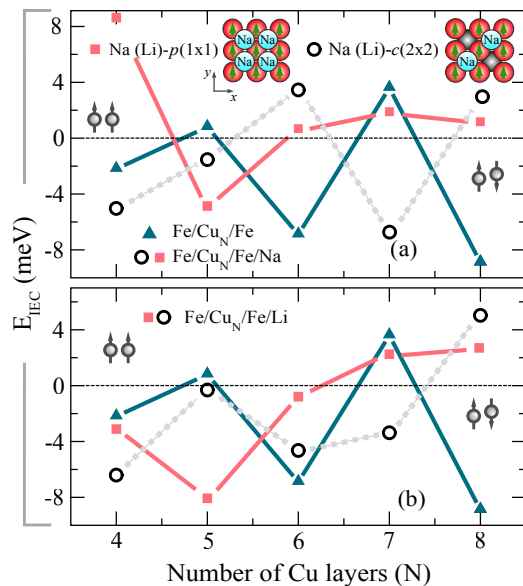


FIG. 2. (Color online) (a) Impact of Na adsorption on the interlayer exchange coupling (IEC) in Fe/Cu_N/Fe (triangles) and Fe/Cu_N/Fe/Na- $p(1 \times 1)$ (squares) for different thickness of Cu spacer. The values of the IEC for $c(2 \times 2)$ configuration of Na (top) on the magnetic layer are represented with circles. The inset shows the $p(1 \times 1)$ and $c(2 \times 2)$ structures of Na or Li adsorbates on the magnetic surface. (b) Similar plot on the variation of the IEC for Fe/Cu_N/Fe and Fe/Cu_N/Fe/Li (rectangles and circles) multilayers with respect to Cu spacer thickness. The IEC of Fe/Cu_N/Fe/Li multilayer with $p(1 \times 1)$ [rectangles] and $c(2 \times 2)$ [circles] configuration of the Li capping layer is also presented.

We have considered two structures of Na (Li) on the Fe surface, namely Na (Li)- $p(1 \times 1)$ and Na (Li)- $c(2 \times 2)$ structures, in order to have more insight on the influence of the Na (Li) coverage on the IEC. The former and latter adsorbate structures covers the magnetic surface fully and partially, respectively. The configuration of these two structures on the magnetic surface is shown in Fig. 2 (a) (see the inset). The Na ions are adsorbed at the hollow site which was identified as the most favorable one for alkali adsorbates^{40,46}. Regarding the magnetic coupling, adsorption of Na ions on the magnetic surface brought an intriguing change to the interlayer exchange coupling. As shown in Fig. 2 (a) (square), when the Fe layer is fully covered with Na [$p(1 \times 1)$] all the magnetic states of Fe/Cu_N/Fe is switched from FM to AF or from AF to FM, except for $N = 7$. Especially a strong change on the IEC, accompanied by magnetic reversal, is observed when the the Cu spacer thicknesses are four and eight. Reducing the Na layer coverage by half, from Na- $p(1 \times 1)$ to Na- $c(2 \times 2)$, can also lead to significant change of the IEC. As shown in Fig. 2 (a) (circles), capping the Fe/Cu_N/Fe multilayer with Na- $c(2 \times 2)$ changes the magnetic order from FM (for the uncapped multilayers) to AF, when the spacer thicknesses are five and seven Cu layers ($N = 5$ and $N = 7$). Moreover, the same configuration of Na varies the interlayer magnetic coupling in Fe/Cu_{6,8}/Fe multilayer from AF to FM one. But, covering the top Fe layer of Fe/Cu₄/Fe with sub-monolayer Na- $c(2 \times 2)$ does not switch the magnetic order. Switching relative magnetic order can be accomplished by increasing the Na coverage, suggesting that the IEC depends on the percentage coverage of Na overlayer. Additional manifestation of the effect of Na coverage on the IEC can be seen on Fe/Cu₇/Fe trilayer. In this multilayer when the Na coverage is reduced by 50 %, from $p(1 \times 1)$ to $c(2 \times 2)$, the IEC changes from 2 meV (FM order) to -7 meV (AF order), respectively. These observations lead us to the conclusion that variations of the IEC induced by Na depends on the configuration of the adsorbate (percentage coverage) as well as on the spacer thickness.

Similar investigations have been done by using Li ions as dopant instead of Na [squares in Fig. 2(b)]. Covering the Fe/Cu_N/Fe structures with single layer of Li- $p(1 \times 1)$ tends to reduce the value of IEC for $N = 7$ and increases the absolute value of the IEC for antiferromagnetically coupled Fe/Cu₄/Fe. Moreover, the magnetic order is reversed from FM (Fe/Cu₅/Fe) to AF (Fe/Cu₅/Fe/Li) when the spacer thickness is five Cu layers. Conversely, for Fe/Cu_{6,8}/Fe trilayers Li doping has the tendency of reducing the strength of AF coupling, and even the relative magnetic order in Fe/Cu₈/Fe is changed to FM coupling (for Fe/Cu₈/Fe/Li), as result of Li doping. In Fig. 2(b)] we have also presented the IEC for Fe/Cu_N/Fe/Li- $c(2 \times 2)$ multilayer, shown in circles. Here reducing the percentage coverage of Li ions from $p(1 \times 1)$ to $c(2 \times 2)$ can only change the strength of the exchange coupling. Only for the case of Fe/Cu₇/Fe/Li- $p(1 \times 1)$ the mutual magnetic order can be switch to AF

coupling by reducing Li coverage [Li- $c(2 \times 2)$] of the magnetic surface. Interestingly, the change on the IEC of FeCu multilayers that are caused by $p(1 \times 1)$ configuration of both Na and Li ions are alike. Moreover, FeCu multilayers that are doped with Na- $c(2 \times 2)$ and Li- $c(2 \times 2)$ also show similar exchange coupling in most cases. All in all, except few cases the trends in which Li or Na ions change the IEC is analogous to one another, implying that similar tuning of the relative magnetization in FM/NM/FM multilayers can also be accomplished by other alkali metals.

V. MAGNETIC HARDENING OF FePt MULTILAYERS WITH Na IONS

We have demonstrated a remarkable effect of direct surface charging and alkali-metal-doping on the interlayer exchange coupling. It is also worthwhile to investigate the impact of Na ions on the magnetic anisotropy energy (MAE) which determines the stability of magnetic systems. In this regard materials with FePt composition are known to have high MAE^{14,47,48} and are used for the current high density recording media⁴⁹. Here, we show that MAE of FePt multilayer can be further enhanced by adsorption of Na ions. In order to verify such way of magnetic hardening effect, we consider a model system which consists of two Fe layers separated with Pt multilayers and theses Fe/Pt_N/Fe stack is supported by Pt(001) substrate. We calculate the MAE as the difference in energy between two axis of magnetization of the system, *i.e.* $MAE = E_x - E_z$. Identical calculation is carried out for Fe/Pt_N bilayer on Pt(001), in order to to estimate the layer resolved MAE and its relation with the interlayer magnetic coupling⁵⁸.

In Fig. 3 (a) the MAE of Fe/Pt_N/Fe trilayer is plotted as function of the Pt spacer thickness, with (squares) and without (circles) the adsorption of Na ions. The values of the MAE are presented for the stable magnetic configurations, and in all cases the easy axis of magnetization is aligned perpendicular to the surface. The FePt multilayers with smaller spacer thicknesses ($N = 2,3$) show high value of MAE relative to the thicker ones. A decrease in the value of the MAE of Fe/Pt_N/Fe is observed when the Pt spacer thickness increases from $N = 3$ to $N = 4$. Further increment of the spacer thickness brings small change to the magnetic anisotropy and an average MAE of 1 meV is observed. As shown in Fig. 3 (b) (circles), for Fe/Pt_{2,5}/Fe the stable magnetic order is found to be ferromagnetic, whereas antiferromagnetic coupling is observed for $N = 3, 4$ and 6. Indeed, the interlayer magnetic order for Fe/Pt₂/Fe is in agreement with similar other systems⁵⁰. Additionally, experimental and theoretical studies have verified the existence of such variation of the interlayer exchange coupling between FM and AF coupling in similar systems^{51,52}.

Basically, Pt is very close to Stoner criterion and can be magnetized when it hybridizes with a ferromagnet.

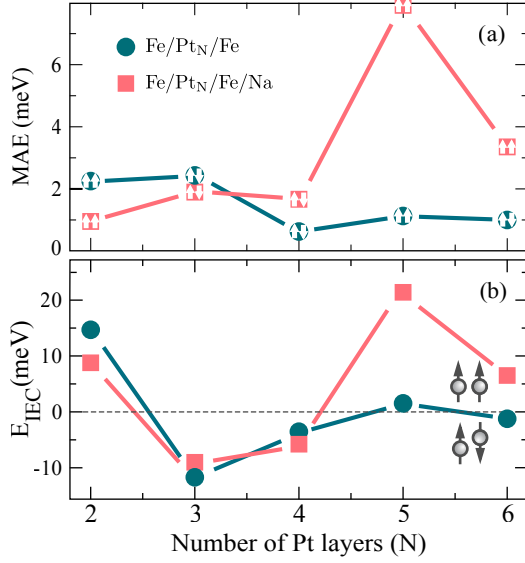


FIG. 3. (Color online) (a) The magnetic anisotropy energy (MAE) of the stable magnetic orders in Fe/Pt_N/Fe (circle) and Na/Fe/Pt_N/Fe (square) for different thickness of Pt spacer is presented. The arrows in the square and circle signs indicate the respective magnetic order for which the magnetic anisotropy is evaluated. (b) The corresponding plot for the interlayer exchange coupling where positive and negative values of the IEC represent ferromagnetic and antiferromagnetic couplings, respectively.

For example, we found that the nearest Pt layer has a magnetic moment up to $0.35 \mu_B$, in Fe/Pt_N/Fe multilayers. In such systems the competition of the induced magnetization from the upper and lower Fe layers determines the magnetic configuration in the neighboring Pt layers, more importantly for $N \leq 3$, and probably the magnetic order within the multilayer. As a consequence of such competition the Fe/Pt_{2,3}/Fe trilayers could be driven away from Stoner instability, leading to antiferromagnetic order. Certainly, the effect of the spin polarized QWS on the IEC still exists, specially for FePt multilayers with thicker Pt spacer. Even more such magnetic coupling can be affected by Na capping layer. For instance, strong change of the IEC is depicted for Fe/Pt_{5,6}/Fe, in Fig. 3 (b), by Na adsorption. Whereas Na capping layer induces moderate change for other FePt multilayers. Additional perspective on the tuning of the IEC in relation to the MAE and Na overlayer are pointed out in the latter part of Sec. VI.

As already mentioned in the earlier sections one of the main goals of this study is to point out the impact of alkali metal deposition on the magnetic anisotropy of FePt thin films. In Fig. 3 (a), contrary to the uncapped multilayers, the FePt multilayers that are capped with Na monolayer show high MAE for thicker spacer thicknesses. Clearly one can see that Na adsorption strongly enhances the MAE when the Pt spacer thicknesses of four, five and six atomic layers. As an example, deposition of Na

ions on Fe/Pt₆/Fe trilayers (AF coupling) significantly enhances the MAE from ~ 1 meV to ~ 3.4 meV, increasing the energy barrier by more than three fold. Exceptionally, for the system whereby the two Fe layers are interspaced with five Pt layer, Na ion capping increase the MAE to ~ 8 meV. Moreover, we have compared the change in the MAE and the IEC and it is clearly seen that the systems with the strongest IEC corresponds to the highest MAE. Specifically, we have already shown that Na deposition strongly increases the IEC of Fe/Pt₅/Fe trilayers from 1.5 meV to 22 meV. The next higher changes in the IEC induced by Na overlayer are observed when the spacer thicknesses of four and six Pt layers are employed. Likewise, the change in the MAE is relatively large. These results clearly hint that the enhancement of the MAE is almost directly related with the absolute value of the change in the interlayer exchange coupling. Moreover, it verifies that the magnetic order and anisotropy of such complex alloy magnetic systems, could be altered as result of ionic doping, leading to a change on the magnetic stability and dynamics^{55,56}. It is experimentally proven fact that the magnetic order of such FM/NM/FM trilayers remains unchanged for thicker ferromagnetic layers^{53,54}, and hence the interplay between the magnetic order and anisotropy.

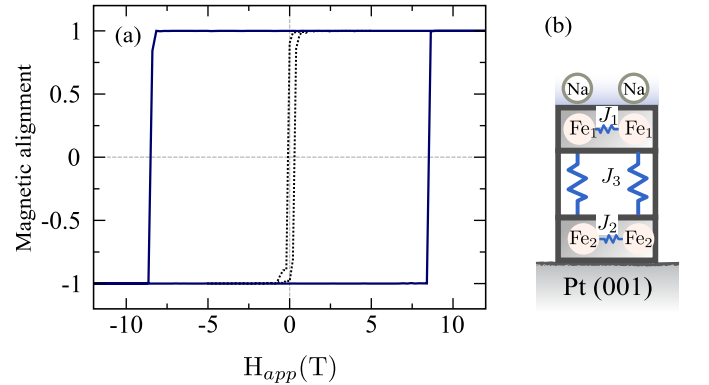


FIG. 4. (Color online) (a) The hysteresis loop of Fe/Pt₅/Fe trilayers with (full lines) and without (dotted lines) Na capping layers. The simulations are performed for out-of-plane direction which is the easy axis of magnetization. (b) An illustrative diagram of the exchange coupling parameters within the multilayer.

Apart from the magnetic properties discussed above the magnetization reversal process is studied by simulating the hysteresis loop for FePt multilayers. In order to do this we apply an external magnetic field within the range of -12 to 12 T. The calculation is performed within the stochastic Landau-Lifshitz-Gilbert (LLG) equation. The LLG equation (Eq. 2) is integrated by using the Heun integration scheme⁵⁷, with a time step of $\Delta t = 1$ fs. The simulations temperature is set to be 5 K. Whereas the damping parameters $\lambda = 1.0$ is used for the sake of computational efficiency. The values of the exchange coupling parameters, J_1 , J_2 and J_3 , as well as the the es-

timated values of the MAE are presented in TABLE I⁵⁸. We have created model system of two Fe layers separated

TABLE I. The exchange parameters [J_1, J_2 and J_3 (meV/ $(\mu_B)^2$)], spin magnetic moments [m_s Fe₁(Fe₂)(μ_B)] and the estimated MAE (in meV) of two Fe layers interspaced with five layers of Pt.

	J_1	J_2	J_3	MAE ₁	MAE ₂	m_s [Fe ₁ (Fe ₂)]
Fe ₂ /Pt ₅ /Fe ₁	5.1	4.9	0.2	0.1	1.2	[2.9 (2.7)]
Fe ₂ /Pt ₅ /Fe ₁ /Na	4.7	4.9	1.4	1.6	6.3	[2.7 (2.9)]

with an effective spacer. Fig. 4 illustrates the hysteresis loops for both FePt multilayers with (full lines) and without (dotted lines) Na deposition. Both multilayers show square like hysteresis loops. One can see that the Na capping layer significantly increase the coercive field to $H_a = \sim 8.5$ T. Therefore, the atomistic spin model simulations clearly demonstrate that alkali metal doping of FePt multilayers favor domain nucleation at elevated temperature by increasing the energy barrier. Furthermore it indicates that magnetic hardening effect can be accomplished by Na ion deposition.

VI. ANALYSIS AND DISCUSSION OF THE RESULTS

The findings that have been discussed until now are supported with analysis on the electronic structure. It is known that the interaction between the magnetic layers is mediated by the confined delocalized electrons in Cu layers^{23,59}, which is a direct consequence of the spin-polarized potential at the Fe/Cu interfaces. Indeed, it is observed that the net charge carriers for negative (positive) charge doping spills (depletes) mainly at the surface, and minimum variation exists below the surface. At this stage there are two factors that can impose changes on the potential of the quantum-well like structure, where the first one is related to the changes in the boundary conditions as a result of the relative alignment of the two magnetic layers, parallel or anti-parallel. Secondly addition or removal of extra charge can alter the Fe/Cu interface as well as the reflectivity of the confined states at the boundaries²³. These two modification will affect the nature of the confinement, being additional scattering constraint of the quantum-well states. In Fig. 5 the effect of these two parameters on the spin polarized quantum-well states (QWSs) of Fe/Cu₄/Fe trilayer is depicted. In these figures the $s+p$ density of states of the coupling medium, for all Cu layers, are plotted for FM (a) and AF (b) coupling. We have considered three charge states, namely positive (q_+), neutral (q_0) and negative (q_-). An electron or hole doping of the order of $1 \bar{e}$ (h) is used for the charged systems. One can infer that the shift of the spin polarized QWS in the energy scale depends on the polarization of the charge doping and consequently this can alter the nature of the

magnetic coupling. For both magnetic orders the positive (negative) charge doping shifts the QWS towards higher (lower) energies. on the other hand, the variation of the magnetic order between the magnetic layers can be directly inferred from the change in the integrated density of state (DOS) which significantly contributes to the total energy^{23,54}, $E = \int^{\varepsilon_F} n(\varepsilon)(\varepsilon - \varepsilon_F)d\varepsilon$, where $n(\varepsilon)$ is the density of states. Thus, the change in the IEC is explained from the shift in the DOS of the magnetic layer or the coupling medium for FM and AF configuration at different charge states. As shown in Fig. 5 the shift of the QWS induced by positive charging is more enhanced for AF coupling. The dependence of such band shift on the magnetic order can lead to stable ferromagnetic coupling in Fe/Cu₄/Fe for positive charging, as it is found in section III. It has to be noted that the QWS are calculated by sampling the k-points near the center of the Brillouin zone. In order to get additional information we also analyzed the total density of states.

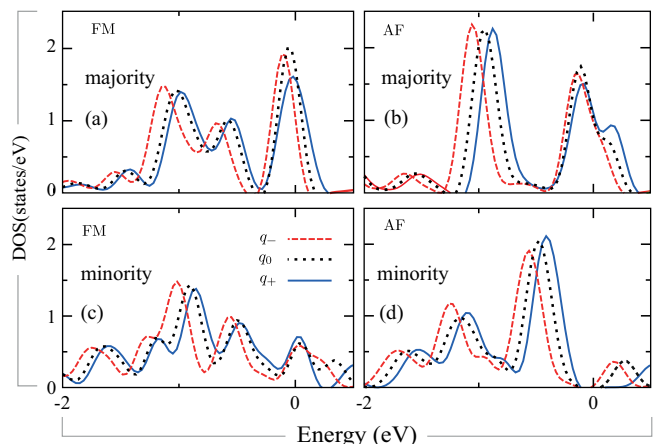


FIG. 5. The spin polarized quantum well states of all Cu spacer layers for FM (a and c) and AF (b and d) orders, at different charge states of the supercell are depicted. The majority and minority DOS are presented on the upper (a and b) and lower (c and d) panel, respectively. The density of states are plotted for positive ($q_+ = 1 h$, blue full line), negative ($q_- = 1 \bar{e}$, red dashed line) and neutral (dotted line) Fe/Cu₄/Fe multilayers, close to the center of Brillouin zone. The vertical dashed line at zero energy level represents the Fermi energy.

Studying the variation of the electronic structure of the top FeCu interface can also provide more insight in the change of the IEC caused by surface charging. First, we would like to focus on the electronic structure of the magnetic layer in order to elucidate the magnetic reversal scenario once more. For both magnetic orders the shift of the minority bands, caused by the surface charging process, show minimum difference and are omitted. Unlike for the case of Cu-QWS (Fig. 5) the majority and minority bands of the Fe layer show opposite shift relative to the neutral system. This leads to an increase or decrease in the exchange splitting as well as the magnetic moment. As shown Fig. 6(a) and (b) the majority QWS

of Cu spacer is shifted to higher energy as Fe/Cu₄/Fe trilayer is positively charged but the majority DOS of Fe are shifted to lower energies. This is caused by the net charge accumulated/depleted and the reflectivity of the confined electrons within the quantum-well like structure (Fe-Cu-Fe) can be modified therewith.

In Fig. 6 (a) and (b) the majority DOS for *d*-orbitals of the top Fe layer, for parallel and anti-parallel alignment, at two different charge states is presented. Similarly, the density of states of the Cu atoms that are interfaced with Fe layer is plotted in Fig. 6 (c) and (d). From these density of states one can infer that there is a hybridization between the *sp* states of Cu with *d*-orbitals of Fe. Explicitly, injecting positive charge of 1 *h* per unit cell induces a strong shift (σ) of the majority *d*-bands of Fe towards the lower energies by $\sigma = 140$ meV and $\sigma = 65$ meV for FM and AF configurations, respectively. This implies that the majority bands of Fe, in the case of ferromagnetic coupling, is more sensitive to positive charge doping which leads to a lower total energy and stable ferromagnetic coupling. The reason for such change of the majority bands is related to the *sp* – *d* hybridization of the Cu layer with top Fe layer. When the system is either negatively or positively charged the *sp* states are affected substantially and it leads to a change in the *sp* – *d* hybridization. Evidently the corresponding shift of the DOS of Cu induced by positive charge doping, to the lower energies, has similar tendency like that of the majority bands of Fe, see Fig. 6 (c) and (d).

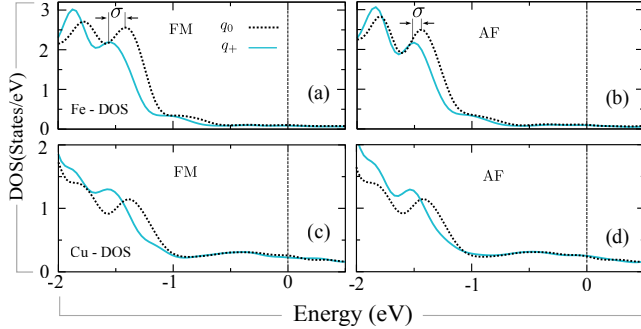


FIG. 6. The majority electron density of states (for *d*-orbitals) of the top Fe layer Fe/Cu₄/Fe, for both FM (a) and AF (b) configurations are shown. The shift in the DOS (σ) are compared for the neutral system and when it is charged with 1.0 *h* per unit cell. The majority density of states for the Cu layer interfaced with top Fe layer is shown in the lower panel. The Cu-DOS is plotted for the cases where Fe/Cu₄/Fe trilayer is coupled ferromagnetically (c) and antiferromagnetically (b). The density of states are integrated over the whole Brillouin zone. The vertical dashed line at zero energy level represents the Fermi energy.

Similar to the case of direct surface charging some insights on the variations of the magnetic order (by alkali metal doping) can be inferred by comparing the QWS and the integrated density of states. However, the mechanism in which the IEC is changed by Na or Li doping in-

volves both chemical and electronic effects, unlike that of direct surface charging. In Fig. 7 the minority quantum well states within the coupling medium of Fe/Cu₄/Fe are calculated near the center of Brillouin zone and presented for FM (a) and AF (b) coupling. In this figure the QWS for both FM and AF orders are displaced to the lower energy as result of Na doping, which is analogous to the case of negative surface charging. Additionally, in Fig. 7 the minority DOS of the top Fe layer in Fe/Cu₄/Fe trilayer is also shown for both FM (c) and AF (d) couplings as well as the DOS of Na capping layers. In both plots, *i.e.* upper panel (Cu-QWS) and lower panel (Fe-DOS) the minority bands are correspondingly shifted to the lower energy as result of Na capping layer. Clearly the effect is more pronounced for the case of FM coupling than the AF ones. Following Na adsorption more states are displaced to the lower energies in the case of FM coupling than AF one, leading to stable FM order. Indeed, similar changes are also observed for the bottom magnetic layer which is mediated by quantum well states. In section IV, we have seen that either reducing the percentage coverage of Na [Na-*c*(2x2)] or Li-*p*(1x1) can reverse the magnetic order of Fe/Cu₄/Fe from AF order to FM order. To get some insight about these differences we have added the minority-DOS plot for top Fe layer [grey dashed line, Fig. 7 (c) and (d)] when the Fe/Cu₄/Fe is doped with Li-*p*(1x1). It seems that Li does not bring strong change to the spin polarized electronic structure of the Fe layer which can induce magnetic reversal. According to Fig. 7 (c) and (d) the shift of the minority bands of Fe to the lower energies by Li-*p*(1x1) overlayer, for FM and AF couplings, is not as pronounced as in the case of Na-*p*(1x1) doping. In the contrary, more minority DOS of Fe layers shifts to lower energy for the case of AF coupling which might only change the value of the exchange coupling.

Once we have discussed the impact of varying the surface electronic structure with surface charging or alkali metal doping. Now, it is important to compare the effects of both surface charging techniques on the IEC. From Fig. 1 and Fig. 2 one can see that covering the magnetic layers with Na-*c*(1x1) does not necessarily lead to similar change like that of electron doping (1 \bar{e} /unit cell). As an example, for Fe/Cu₄/Fe trilayer electron doping and Na [Na-*c*(1x1)] deposition have opposite effect relative to the neutral system. However, the impact of the submonolayer Na-*c*(2x2) and the direct surface charging techniques consistently favors the same magnetic orders for almost all Cu spacer thickness.

Using atomistic spin model simulations, perhaps for the first time we revealed magnetic hardening mechanism in FePt multilayers by Na ion doping. These variations in the MAE are mainly caused by a combined effect of the interlayer exchange coupling and the changes in surface electronic structure induced by Na. In order to elucidate the first case we compared the MAE for three different cases, *i.e.* Fe/Pt₅, Fe/Pt₅/Fe and Fe/Pt₅/Fe/Na on Pt(001). The MAE of the first structure is found to

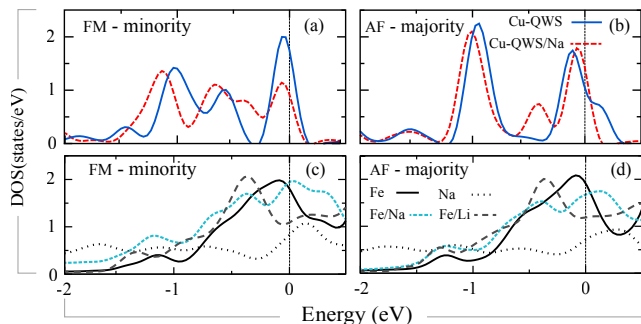


FIG. 7. The effect of Na capping layer in the confined states of the quantum well like structure, Fe/Cu₄/Fe. The DOS of the QWS are presented for minority states with [(a), full line] and without Na doping [(b), dashed line]. The minority electronic density of states (for *d*-orbitals) of Fe depicted without (full lines) and with (dashed lines) adsorption of Na ions. All the DOSs are plotted for the top Fe layer within the FM (c) and AF (d) configurations of Fe/Cu₄/Fe. The dashed gray line shows the minority bands of the top Fe in Fe/Cu₄/Fe/Li-*p*(1x1) multilayer. The DOS for the Na layer is also shown in dotted lines and it is multiplied by factor of ten. Since the shift of the majority DOS as result of Na ion doping is relatively similar, for both FM and AF order, and are not included. The vertical dashed line at zero energy level represents the Fermi energy.

be 1.6 meV. When the bilayer Fe/Pt₅ is terminated with Fe layer (Fe/Pt₅/Fe), it leads to the onset of the effect of interlayer exchange coupling on the magnetic anisotropy. The added (top) magnetic layer which couples ferromagnetically with the bottom Fe layer brings small change to the MAE. However, deposition of Na ion increases the MAE enormously. Here the strong change of the MAE is the ramifications of the IEC and the change in the electronic structure of the FePt interfaces. This implies that both the magnetic order and the interface electronic structure are relevant parameters that could possibly affect the MAE by varying the spin-orbit coupling. Essentially, the contribution of the spin-orbit coupling to each axis of magnetization, in-plane or out-of plane, determines the MAE. For instance, in FePt multilayers the coupling between occupied and unoccupied states of d_δ and d_π orbitals are identified as the dominant ones among the minority *d*-orbitals^{47,60}, where $d_\delta = d_{x^2-y^2} + d_{xy}$ and $d_\pi = d_{xz(yz)} + d_{z^2}$. For the case of Fe/Pt₅/Fe/Na the orbitals d_δ (d_π) are less (more) degenerate near to the Fermi energy for the top Fe layer as compared to the lower ones. This tends to lower the energy when the magnetization of the multilayer is perpendicular to the surface, leading to a substantial increase in the MAE for the bottom FePt interfaces. In addition the magnetic moment as well as the induced magnetic moment for the lower FePt interfaces has increased as result of Na capping, and conversely reduces for top layers.

On the other hand some of the FePt multilayers with high MAE have stable antiferromagnetic coupling, implying that these FePt thin films could be essential can-

didates for AF domains⁶¹. Besides, AF domains have highly minimized dipolar magnetic interaction between the neighboring bits, and could play a crucial role in reducing the density of the current magnetic storage device⁴⁹. Additionally such AF multilayers can be an integral part of an exchange biased system and could have significant impact in the quest of ultra-fast magnetic switching^{55,56}. In fact, the switching procedure of the relative magnetization by incorporating alkali-metal doping can also be perceived as follows. Regardless of the original magnetic order in FM/NM/FM trilayer, first one has to overcome the energy barrier (MAE) of the top ferromagnet in order to switch to the opposite direction. The magnetic anisotropy of each magnetic layer in FePt multilayer is estimated in the earlier section. This energy barrier can certainly be altered by introducing alkali metal in to the system, which varies the interface electronic structure. The charge rearrangements are then transformed to magnetic anisotropy through spin-orbit coupling which results in changes of the relative orientation of the atomic moments. But both surface charging techniques does not always lead to magnetization reversal. Instead, a favorable conditions will be created for other means of spin manipulation mechanisms, *e.g.* spin transfer torque^{7,8} or electrostatic gating^{37,62,63}, leading to switching mechanism assisted with alkali metal doping. Therefore, once the energy barrier is completely overcome the system probably settles down to the reversed state.

VII. CONCLUSION

In summary, we have presented a comprehensive study which reveals the effect of two surface-interface charging techniques on the IEC of magnetic layers across Cu and Pt spacers as well as their MAE. Explicitly, in some cases the mutual magnetic orders of fully metallic FM/NM/FM-like structure can be remarkably tuned between ferromagnetic and antiferromagnetic states by addition or removal of extra charge. Moreover, employing alkali metals as dopants we have shown a natural way of space charge alteration mechanism which can reverse the relative magnetic orders in alloyed multilayers and strongly enhance the MAE of Fe/Pt. These effect leads us to the conclusion that alkali-metal-induced charging magnetic surfaces can assist the process of magnetization reversal and also controlling the spin states as well as the spin dynamics. All in all, our findings suggest that involving alkali metals in field of spintronics could have significant impact in order to control and design new functional spintronic devices or quantum computing.

VIII. ACKNOWLEDGMENT

T. R. Dasa would like to acknowledge Richard F. L. Evans at the University of York for the helpful discussion

related to the atomistic model approach. We would also like to thank O. O. Brovko and P. Ruiz-Díaz for the fruit-

ful discussion. This work is supported by the Deutsche Forschungsgemeinschaft (DFG) within the SFB 762.

- ¹ E. Y. Tsybal, Electric toggling of magnets, *Nature Materials* **11**, 12 (2012).
- ² N. A. Spaldin, and M. Feibig, The renaissance of magnetoelectric multiferroics, *Science* **309**, 391 (2005).
- ³ F. S. G. Binasch, P. Grunberg, and W. Zinn, Enhanced magnetoresistance in layered magnetic structures, *Phys. Rev. B* **39**, 4828 (1989).
- ⁴ M. N. Baibich, J. M. Broto, A. Fert, F. Nguyen Van Dau, F. Petroff, P. Eitenne, G. Creuzet, A. Friederich, and J. Chazelas, Giant magnetoresistance of (001)Fe/(001)Cr magnetic superlattices, *Phys. Rev. Lett.* **61**, 2472 (1988).
- ⁵ S. S. P. Parkin, C. Kaiser, A. Panchula, P. M. Rice, B. Huges, M. Samant, and S.-H. Yang, Giant tunneling magnetoresistance at room temperature with MgO (100) tunnel barriers, *Nature Mater.* **3** 862-867 (2004).
- ⁶ M. Kryder, and C. S. Kim, After hard drives what comes next?, *IEEE Transactions on Magnetics* **45**, 3406, (2009).
- ⁷ J. Slonczewski, Current-driven excitation of magnetic multilayers, *JMMM* **159**, L1-L7 (1996).
- ⁸ L. Berger, Emission of spin waves by magnetic multilayer traversed by a current, *Phys. Rev. B* **54**, 9353 (1996).
- ⁹ W. G. Wang, and C. L. Chien, Voltage-induced switching in magnetic tunnel junctions with perpendicular magnetic anisotropy, *J. Phys. D: Appl. Phys.* **46** 074004 (2013).
- ¹⁰ J. Zhu, J. A. Katine, Graham E. Rowlands, Y.-J. Chen, Z. Duan, J. G. Alzate, P. Upadhyaya, J. Langer, P. K. Amiri, K. L. Wang, and I. N. Krivorotov, Voltage-induced ferromagnetic resonance in magnetic tunnel junctions, *Phys. Rev. Lett.* **108**, 197203 (2012).
- ¹¹ H. C. Wu, O. N. Mryasov, M. Abid, K. Radican Igor, and V. Shvets Magnetization states of all-Oxide spin valves controlled by charge-orbital ordering of coupled ferromagnets, *Sci. Rep.* **3**, 1830 (2013).
- ¹² K. Nakamura, R. Shimabukuro, Y. Fujiwara, T. Akiyama, T. Ito, and A. J. Freeman, Giant modification of the magnetocrystalline anisotropy in transition-metal monolayers by an external electric field, *Phys. Rev. Lett.* **102**, 187201 (2009).
- ¹³ O. O. Brovko, P. Ruiz-Díaz, T. R. Dasa, and V. S. Stepanyuk, Controlling magnetism on metal surfaces with non-magnetic means : electric fields and surface charging, *J. Phys.: Condens. Matter* **26**, 093001 (2014).
- ¹⁴ M. Tsujikawa and T. Oda, Finite Electric Field Effects in the Large Perpendicular Magnetic Anisotropy Surface Pt/Fe/Pt(001): A First-Principles Study, *Phys. Rev. Lett.* **102**, 247203 (2009).
- ¹⁵ P. Ruiz-Díaz, T. R. Dasa, and V. S. Stepanyuk, Tuning magnetic anisotropy in metallic multilayers by surface charging: an *ab-initio* study *Phys. Rev. Lett.* **110**, 267203 (2013).
- ¹⁶ S. Subkow, and M. Fähnle, Electron theory of magnetoelectric effects in metallic ferromagnetic nanostructures, *Phys. Rev. B* **84**, 054443 (2011).
- ¹⁷ S Sahoo, S. Polisetty, C.-G. Duan, S. Jaswal, E. Tsybal, and C. Binck, Ferroelectric control of magnetism in BaTiO₃/Fe heterostructures via interface strain coupling, *Phys. Rev. B* **76**, 092108 (2007).
- ¹⁸ A. Sonntag, J. Hermenau, A. Schlenhoff, J. Friedlein, S. Krause, and R. Wiesendanger, Electric-field-induced magnetic anisotropy in a nanomagnet investigated on the atomic Scale, *Phys. Rev. Lett.* **112** 017204 (2014).
- ¹⁹ C. Bi, Y. Liu, T. Newhouse-Illige, M. Xu, M. Rosales, J. W. Freeland, O. Mryasov, S. Zhang, S. G. E. te Velthuis, and W. G. Wang, Reversible control of Co magnetism by voltage-induced oxidation, *Phys. Rev. Lett.* **113**, 267202 (2014).
- ²⁰ N. A. Pertsev, and H. Kohlstedt, Resistive switching via the converse magnetoelectric effect in ferromagnetic multilayers on ferroelectric substrates, *Nanotechnology* **21** 475202 (2009).
- ²¹ J. T. Heron, M. Trassin, K. Ashraf, M. Gajek, Q. He, S. Y. Yang, D. E. Nikonov, Y.-H. Chu, S. Salahuddin, and R. Ramesh, Electric-field-induced magnetization reversal in a ferromagnet-multiferroic heterostructure, *Phys. Rev. Lett.* **107**, 217202 (2011).
- ²² M. Fechner, P. Zahn, S. Ostanin, M. Bibes, and I. Mertig, Switching magnetization by 180 with an electric Field, *Phys. Rev. Lett.* **108**, 197206 (2012).
- ²³ P. Bruno, and C. Chappert, Ruderman-Kittel theory of oscillatory interlayer exchange coupling, *Phys. Rev. B* **46**, 261 (1992).
- ²⁴ W.-S. Zhang, B. Z. Li, and Y. Li, Conductance, magnetoresistance, and interlayer exchange coupling in magnetic tunnel junctions with nonmagnetic metallic spacers and finite thick ferromagnetic layers, *Phys. Rev. B* **58**, 14959 (1998).
- ²⁵ G. Kresse, and D. Joubert, From ultrasoft pseudopotentials to the projector augmented-wave method, *Phys. Rev. B* **59**, 1758 (1999).
- ²⁶ G. Kresse, and J. Hafner, Ab initio molecular dynamics for liquid metals *Phys. Rev. B* **47**, 558 (1993).
- ²⁷ G. Kresse, and J. Furthmüller, Efficient iterative schemes for ab initio total-energy calculations using a plane-wave basis set, *Phys. Rev. B* **54**, 11169 (1996).
- ²⁸ D. M. Ceperley, and B. J. Alder, Ground state of the electron gas by a stochastic method, *Phys. Rev. Lett.* **45**, 566 (1980).
- ²⁹ The layers in the slabs are initially interspaced with a bulk interlayer distance of 1.95 Å, associated with the calculated lattice constant of fcc Pt (3.91 Å). Later on the geometry of the system is relaxed until the force on each atom to the surface is less than 5 meV/Å. The Fe/Cu(Pt)/Fe layers are supported by a substrate which consists of ten Pt layers.
- ³⁰ G. Makov, and M. C. Payne, Periodic boundary conditions in ab initio calculations, *Phys. Rev. B* **51**, 4014 (1995).
- ³¹ G. Kresse and O. Lebacqz, VASP Manual, [http : //cms.mpi.univie.ac.at/vasp/vasp/](http://cms.mpi.univie.ac.at/vasp/vasp/)
- ³² R. F. L. Evans, W. J. Fan, P. Chureemart, T. A. Ostler, M. O. A. Ellis, and R. W. Chantrell, Atomistic spin model simulations of magnetic nanomaterials, *J. Phys.: Condens. Matter* **26**, 103202 (2014). [http : //vampire.york.ac.uk/](http://vampire.york.ac.uk/)
- ³³ W. F. Brown, Thermal fluctuations of a single-domain particle, *Phys. Rev.* **130**, 1677 (1963).

- ³⁴ Electron charge is represented with ' \bar{e} ' whereas ' h ' depicts a hole charge, being $-\bar{e}$. Similarly arbitrary positive and negative charge concentration within the multilayers are depicted with q_+ and q_- signs respectively. The parameters that are employed to calculate the MAE and IEC are tested for their reliability which could result in an insignificant of our results. For instance, for Fe/Pt₃/Fe, increasing the number of k -point to 25x25x1 (where cutoff energy = 430 eV) the MAE varies only by 6%, relative to the one reported in the paper. Additionally, when the k -point and plane wave cutoff energy are 21x21x1 and 500 eV, respectively, the MAE changes only by 3%.
- ³⁵ M. Weisheit, S. Fhler, A. Marty, Y. Souche, C. Poinsignon, and D. Givord, Electric field-induced modification of magnetism in thin-film ferromagnets, *Science* **315** 349 (2007).
- ³⁶ H. Zhang, M. Richter, K. Koepf, I. Opahle, F. Tasnádi, and H. Eschrig, Electric-field control of surface magnetic anisotropy: a density functional approach, *New J. Phys.* **11**, 043007 (2009).
- ³⁷ T. Maruyama, Y. Shiota, T. Nozaki, K. Ohta, N. Toda, M. Mizuguchi, A. A. Tulapurkar, T. Shinjo, M. Shiraishi, S. Mizukami, Y. Ando and Y. Suzuki, Large voltage-induced magnetic anisotropy change in a few atomic layers of iron, *Nature nanotechnology* **4**, 158 (2009).
- ³⁸ C. Krull, R. Robles, A. Mugarza, and P. Gambardella, Site- and orbital-dependent charge donation and spin manipulation in electron-doped metal phthalocyanines, *Nature Mater.* **12** 337 (2013).
- ³⁹ J. Repp, G. Meyer, F. E. Olsson, and M. Persson, Controlling the charge state of individual gold adatoms, *Science* **305** 493 (2004).
- ⁴⁰ G. Fratesi, Potential energy surface of alkali atoms adsorbed on Cu(001), *Phys. Rev. B* **80**, 045422 (2009).
- ⁴¹ A. N. Rudenko, F. J. Keil, M. I. Katsnelson, and A. I. Lichtenstein, Exchange interactions and frustrated magnetism in single-side hydrogenated and fluorinated graphene, *Phys. Rev. B* **88**, 081405(R) (2013).
- ⁴² M. Cinchetti, S. Neuschwander, A. Fischer, A. Ruffing, S. Mathias, J.-P. Wüstenberg, and M. Aeschlimann, Tailoring the spin functionality of a hybrid metal-organic interface by means of Alkali-metal doping, *Phys. Rev. Lett.* **104**, 217602 (2010).
- ⁴³ J. Zhao, N. Pontius, A. Winkelmann, V. Sametoglu, A. Kubo, A. G. Borisov, D. Sanchez-Portal, V. M. Silkin, E. V. Chulkov, P. M. Echenique, and H. Petek, Electronic potential of a chemisorption interface, *Phys. Rev. B* **78**, 085419 (2008).
- ⁴⁴ J. Mathon, M. Villeret, A. Umerski, R. B. Muniz, J. d'Albuquerque e Castro, and D. M. Edwards, Quantum-well theory of the exchange coupling in magnetic multilayers with application to Co/Cu/Co(001), *Phys. Rev. B* **56**, 11797 (1997).
- ⁴⁵ M. Kowalewski, B. Heinrich, T. C. Schulthess, and W. H. Butler, First principles calculations of interlayer exchange coupling in bcc Fe/Cu/Fe structures, *IEEE Transactions on Magnetics* **34**, 1225 (1998).
- ⁴⁶ Yamauchi Y, Kurahashi M, Suzuki T and Ju X, Influence of submonolayers of sodium on the spin polarization of iron outmost surfaces, *J. Appl. Phys.* **93**, 8734 (2009).
- ⁴⁷ T. R. Dasa, P. Ruiz-Díaz, O. O. Brovko and V. S. Stepanyuk, Tailoring magnetic properties of metallic thin films with quantum well states and external electric fields, *Phys. Rev. B* **88**, 104409 (2013).
- ⁴⁸ J. B. Staunton, S. Ostanin, S. S. A. Razee, B. L. Gyorffy, L. Szunyogh, B. Ginatempo, and E. Bruno Temperature dependent magnetic anisotropy in metallic magnets from an *abinitio* electronic structure theory: L1₀-ordered FePt, *Phys. Rev. Lett.* **93**, 257204 (2004).
- ⁴⁹ T. Klemmer, N. Shukla, C. Liu, X. Wu, E. Svedberg, O. Mryasov, R. Chantrell, D. Weller, M. Tanase and D. Laughlin, Structural studies of L10 FePt nanoparticles, *Appl. Phys. Lett.* **81** 2220 (2002).
- ⁵⁰ L. V. Dzemiantsova, M. Hortamani, C. Hanneken, A. Kubetzka, K. von Bergmann, and R. Wiesendanger, Magnetic coupling of single Co adatoms to a Co underlayer of variable thickness, *Phys. Rev. B* **86**, 094427 (2012).
- ⁵¹ F. Yildiz, M. Przybylski, and J. Kirschner, Direct evidence of a nonorthogonal magnetization configuration in single crystalline system, *Phys. Rev. Lett.* **103**, 147203 (2009).
- ⁵² S. Blizak, G. Bihlmayer, S. Blügel, and S. E. H. Abaidia, Interlayer exchange coupling between FeCo and Co ultrathin films through Rh(001) spacers, *Phys. Rev. B* **91**, 014408 (2015).
- ⁵³ P. J. H. Bloemen, M. T. Johnson, M. T. H. van de Vorst, R. Coehoorn, J. J. de Vries, R. Jungblut, J. van de Stegge, A. Reinders, and W. J. M. de Jonge, Magnetic layer thickness dependence of the interlayer exchange coupling in (001) Co/Cu/Co, *Phys. Rev. Lett.* **72**, 764 (1994).
- ⁵⁴ P. Lang, L. Nordström, K. Wildberger, R. Zeller, P. H. Dederichs, and T. Hoshino, Ab initio calculations of interaction energies of magnetic layers in noble metals: Co/Cu(100), *Phys. Rev. B* **53**, 9092 (1996).
- ⁵⁵ I. Radu, K. Vahaplar, C. Stamm, T. Kachel, N. Pontius, H. A. Dürr, T. A. Ostler, J. Barker, R. F. L. Evans, R. W. Chantrell, A. Tsukamoto, A. Itoh, A. Kirilyuk, Th. Rasing and A. V. Kimel, Transient ferromagnetic-like state mediating ultrafast reversal of antiferromagnetically coupled spins, *Nature* **472**, 205 (2011).
- ⁵⁶ A. V. Kimel, A. Kirilyuk, A. Tsvetkov, R. V. Pisarev, and Th. Rasing Laser-induced ultrafast spin reorientation in the antiferromagnet TmFeO₃, *Nature* **429**, 850 (2004).
- ⁵⁷ U. Nowak, in *Annual Reviews of Computational Physics IX* (World Scientific, Singapore, 2001), p. 105.
- ⁵⁸ Independent calculation are done in order to find the exchange parameters J_1 and J_2 from the supercell Pt(001)/Fe/(Na) and Pt(001)/Fe/Pt₅ respectively. Based on the number of nearest neighbors (N_n) and the magnetic moments (m_i, m_j) of the interacting spins, the parameters are determined according to $E_{AF} - E_{FM} = 2N_n J_{ij} m_i m_j$. Regarding the MAE, first we calculate MAE of Pt(001)/Fe/Pt₅ and Pt(001)/Fe/Pt₅/Fe/Na multilayers, separately. Then we took difference in the MAE of these multilayers, the changes in the spin and orbital moments and analysis on the DOS (based on second order perturbation theory⁶⁰) in order to estimate of the MAE of each magnetic layer.
- ⁵⁹ O. Brovko, P. Ignatiev, V. Stepanyuk and P. Bruno, Tailoring exchange interactions in engineered nanostructures: an *ab-initio* study, *Phys. Rev. Lett.*, **101**, 036809 (2008).
- ⁶⁰ D. S. Wang, R. Wu, and A. J. Freeman, First-principles theory of surface magnetocrystalline anisotropy and the diatomic-pair model, *Phys. Rev. B* **47**, 14932 (1993).
- ⁶¹ Nolting F, A. Scholl, J. Stöhr, J. W. Seo, J. Fompeyrine, H. Siegwart, J.-P. Locquet, S. Anders, J. Lüning, E. E. Fullerton, M. F. Toney, M. R. Scheinfein, and H. A. Padmore, Direct observation of the alignment of ferromagnetic spins by antiferromagnetic spins, *Nature* **405**, 767 (2000).

- ⁶² U. Bauer, M. Przybylski, and G. S. D. Beach, Voltage control of magnetic anisotropy in Fe films with quantum well states, *Phys. Rev. B* **89**, 174402 (2014).
- ⁶³ K. Shimamura, D. Chiba, S. Ono, S. Fukami, N. Ishiwata, M. Kawaguchi, K. Kobayashi, and T. Ono, Electrical control of Curie temperature in cobalt using an ionic liquid film, *Appl. Phys. Lett.* **100** 122402 (2012).